Author/s:
Gustafsson, OJR;Guinan, TM;Rudd, D;Kobus, H;Benkendorff, K;Voelcker, NH

Title:
Metabolite mapping by consecutive nanostructure and silver-assisted mass spectrometry imaging on tissue sections

Date:
2017-06-30

Citation:
Gustafsson, O. J. R., Guinan, T. M., Rudd, D., Kobus, H., Benkendorff, K. & Voelcker, N. H. (2017). Metabolite mapping by consecutive nanostructure and silver-assisted mass spectrometry imaging on tissue sections. Rapid Communications in Mass Spectrometry, 31 (12), pp.991-1000. https://doi.org/10.1002/rcm.7869.

Persistent Link:
https://hdl.handle.net/11343/292913

Metabolite mapping by consecutive nanostructure and silver-assisted mass spectrometry imaging on tissue sections

O. J. R. Gustafsson[1]†, T. M. Guinan[1]†, D. Rudd[2], H. Kobus[3], K. Benkendorff[2], and N. H. Voelcker[1]*

[1] Australian Research Council Centre of Excellence in Convergent Bio-Nano Science and Technology, Future Industries Institute, University of South Australia, Mawson Lakes, South Australia, Australia 5095.
[2] School of Environment, Science and Engineering, Southern Cross University, Lismore, New South Wales, Australia 2480.
[3] School of Chemical and Physical Sciences, Flinders University, Bedford Park, South Australia, Australia 5042.

† Both authors contributed equally.

* Corresponding author: nico.voelcker@unisa.edu.au

RATIONALE: Nanostructure-based mass spectrometry imaging (MSI) is a promising technology for molecular imaging of small molecules, without the complex chemical background typically encountered in matrix-assisted molecular imaging approaches. Here, we have enhanced these surfaces with silver (Ag) to provide a second tier of MSI data from a single sample.
METHODS: MSI data was acquired through the application of laser desorption/ionization mass spectrometry to biological samples imprinted onto desorption/ionisation on silicon (DIOS) substrates. Following initial analysis, ultra-thin Ag layers were overlaid onto the samples followed by MSI analysis (Ag-DIOS MSI). This approach was first demonstrated for fingermark small molecules including environmental contaminants and sebum components. Subsequently, this bimodal method was translated to lipids and metabolites in fore-stomach sections from a 6-bromoisatin chemopreventative murine mouse model.
RESULTS: DIOS MSI allowed mapping of common ions in fingermarks as well as 6-bromoisatin metabolites and lipids in murine fore-stomach. Furthermore, DIOS MSI was complemented by the theAg-DIOS MSI of Ag-adductable lipids such as wax esters in fingermarks and cholesterol in murine forestomach. Gastrointestinal acid condensation products of 6-bromoisatin, such as the 6,6'-dibromoindirubin mapped herein, are very challenging to isolate and characterize. By re-analysing the same tissue imprints, this metabolite was readily detected by DIOS, placed in a tissue-specific spatial context, and subsequently overlaid with additional lipid distributions acquired using Ag-DIOS MSI.
CONCLUSIONS: The ability to place metabolite and lipid classes in a tissue-specific context makes this novel method suited to MSI analyses where the collection of additional information from the same sample maximises resource use, and also maximises the number of annotated small molecules, in particular for metabolites that are typically undetectable with traditional platforms.

Key words: DIOS • imaging • silver • fingermark • stomach

This is the author manuscript accepted for publication and has undergone full peer review but has not been through the copyediting, typesetting, pagination and proofreading process, which may lead to differences between this version and the Version of Record. Please cite this article as doi: 10.1002/rcm.7869

INTRODUCTION

Mass spectrometry imaging (MSI) provides a capacity for mapping biological analytes in animal tissues [1-5], botanical samples [3] and even fingermarks [6, 7]. The unique advantages of MSI include the ability to simultaneously annotate the spatial distribution of hundreds to thousands of analytes, without the need for specific and costly reagents such as antibodies [8]. With separately tailored sample preparation methods, MSI can spatially annotate small molecules (drugs/lipids) as well as peptides or proteins, including those with post-translational modifications. As thin (μm) tissue sections are typically used, this technology is ideally suited for application to materially limited samples [4]: a strength which can be exploited further by applying multiple rounds of analysis to the same sample section [9-11]. These multimodal methods are opening new vistas that will allow MSI to become a truly global profiling method for the multiple analyte classes which exist in biological samples, thereby allowing a measure of spatial integration for the varied "omics" fields (metabolomics, lipidomics, proteomics). To achieve this with traditional analytical platforms requires many grams of tissue and a significant investment of time, employing separation strategies.

Typical MSI methodologies use matrix-assisted laser desorption/ionization (MALDI) to produce gaseous ions for MS [12]. However, the interference of matrix ions in the low mass range (< *m/z* 1000), and the exacting sample preparation methods required for matrix-assisted methods, have led to increasing use of matrix-free strategies, including sputtered metals [7, 13], nanoparticles (NPs) [14] and nanostructured substrates [6]. One of the most successful of these is desorption/ionization on silicon (DIOS), which uses a perfluorinated porous silicon (pSi) substrate [15]. The high surface area (up to 800 m^2/g) and UV absorptivity of pSi [16-18] allow it to replace matrix compounds for laser desorption/ionization (LDI) measurement of small molecules. DIOS substrates are known to be robust analytical surfaces for fingermarks [6], the material left behind following finger contact with a surface, which can include environmental (detergents, explosives) and endogenous (drugs, lipids) compounds [19]. However, DIOS analysis of some analytes including fatty acids (FAs) is often difficult due to a lack of available protonation sites. Thus, negative ion mode has been used for the DIOS analysis of FAs as deprotonation is a more favourable process [20, 21]. If multiple analyses are required, to capture a greater set of ions from tissue, there is benefit in enhancing the detection of a greater or different set of analytes by combining DIOS with silver (Ag)-assisted DIOS (Ag-DIOS) [22] - as a secondary ionization method rather than working on a different section of tissue. Ag is a well-known cationization agent for FAs and esters [20, 23] and, when applied to MALDI time-of-flight (MALDI-ToF) MS platforms where mass accuracy is intrinsically married to sample preparation quality (i.e. homogeneity), it produces a high level of mass accuracy by allowing internal calibration of mass spectra [7, 22]. In addition, the coating of Ag onto substrates has enhanced the detection of sterols, wax esters (WEs) and triacylglycerols (TAGs) [2, 3, 13, 23], lipid classes that are challenging to analyze via DIOS and for typical MS characterization approaches require derivatization prior to detection of ion adducts[24].

Here, we present the first consecutive usage of DIOS and Ag-DIOS to realize dual MSI analysis of both fingermarks and tissue sections. The ion distributions for fingermark compounds and tissue metabolites of 6-bromoisatin were mapped with DIOS, and endogenous lipid distributions were mapped using consecutive DIOS and Ag-DIOS MSI. Traditional lipid histochemical techniques as well as emerging techniques for vibrational microscopy (e.g. Raman scattering) do not achieve the molecular specificity of MS and immune- and fluorescently-labelled methods require *a priori* knowledge of the target lipid metabolite [25]. Using the combined DIOS/Ag-DIOS pipeline (Fig. 1) additional mass spectral information was obtained with reduced spectral noise in the low mass range, high mass accuracy, and enhanced detection of small molecules with low ionization efficiency (FAs,

cholesterol). Consecutive DIOS/Ag-DIOS is thus likely to improve the spatial mapping of small molecules in animal models.

. -

EXPERIMENTAL

Chemicals and biological samples

Hydrofluoric acid (HF, 48%) and undenatured ethanol (99.9%) were purchased from Scharlau Chemie (Chem-Supply, Gillman, Australia). Tridecafluoro-1,1,2,2-tetrahydrooctyl-dimethylchlorosilane (F_{13}) was purchased from Gelest (Morrisville, PA, USA). Mouse stomach was obtained from a colorectal cancer early stage tumor model under Flinders University animal welfare approval 751-10. Briefly, 10-week old C57BL/6J mice (Animal Resources Centre, Perth, Australia) were treated as follows: 6-bromoisatin (0.05 mg/g) was administered by daily oral gavage in 100 µL sunflower oil medium, for fourteen weeks in total. After two weeks, 10 mg/kg azoxymethane (AOM) was administered by six peritoneal injections (one week apart – six weeks total). Oral gavage was continued for a further six weeks, followed by a single 6-bromoisatin gavage (four hours before sacrifice) to allow detection of the compound and its metabolites in the gastrointestinal tract. Mice were euthanized and sacrificed by cervical dislocation prior to dissection to remove the stomach, which was frozen in liquid nitrogen and stored at -80°C.

Preparation of DIOS substrates, fingermark deposition and tissue section mounting

DIOS substrates were prepared as previously described [6]. The second digit (unwashed index finger) was placed in contact with the substrate for 5 s. Tissue sections (14 µm) were sectioned on a CM1800 cryotome (Leica, Waverley, Australia), thaw mounted onto a DIOS substrate and stored at -80°C until analysis. For analysis, the substrate was thawed and the tissue section rinsed off the surface using a stream of deionized water [26, 27]. All substrates were scanned (4800 dpi) using an Epson Perfection V600 flatbed scanner (Officeworks, Australia). Double-sided carbon tape was used to fix substrates to a custom MTP-384 target plate (Bruker Daltonics, Bremen, Germany).

Ag-DIOS preparation

The DIOS substrates were immediately sputter-coated with a 1.4 nm thick Ag layer (99.9999% purity) using a Q300T-D sputter coater (Quorom Technologies, Laughton, UK) operating at 50 mA with a quartz crystal micro-balance (tooling factor – 8.5) for layer thickness estimation.

Mass spectrometry, data processing and presentation

All MSI acquisitions were performed in reflectron positive mode on an ultrafleXtreme MALDI-ToF/ToF instrument (Bruker Daltonics) at 60 µm spatial resolution. Instrument specific settings were as follows, reflector gain: 2.651 kV, repetition rate: 2 kHz, shots per position: 600, ion source voltage 1: 20 kV, ion source voltage 2: 17.55 kV, lens voltage: 7.6 kV, reflector voltage 1: 21.1 kV and reflector voltage 2: 10.95 kV. Data acquisition used flexControl 3.4.78 (Bruker Daltonics) and flexImaging 3.4 (Bruker Daltonics). The laser fluence was optimized by the operator. Pre-MSI calibration used a 50:50 mix of 10 mg/mL CsI and 10 mg/mL trans-2-[3-(4-tert-Butylphenyl)-2-methyl-2-propenylidene]malononitrile (DCTB) in ethanol. MS/MS spectra were acquired using a proprietary "LIFT" method and processed in flexAnalysis (3.4, Bruker Daltonics). Ag-DIOS pre- and internal calibration used Ag clusters [22]. The spectra were processed in flexImaging, flexAnalysis, SCiLS (SCiLS, Bremen, Germany) and R [28]. The data processing and supplementary methods are described in the Supporting Information.

RESULTS and DISCUSSION

Fingermarks were selected for initial development and testing of the DIOS/Ag-DIOS MSI method, primarily as fingermarks contain a broad range of small molecule classes, including environmental contaminants (ditallow dimethyl ammonium chloride, DTDMAC), lipids (FAs, TAGs), sterols and WEs. Furthermore, as the fingermark only has to be contact deposited, sample preparation is straightforward and rapid. Finally, any improvements in the set of fingermark ions detected by the combined MSI method have direct inter-disciplinary impact on forensic analysis. This is most relevant for the collection of control prints by law enforcement agencies [19], as these prints could be deposited onto any surface, including DIOS. For example, rapid analysis of small regions on these collected fingermarks could be used for the detection of illicit drugs [6].

Two fingermarks were thus independently deposited onto identical DIOS substrates and analyzed by DIOS MSI. Only half of each fingermark was analyzed by MSI: this allowed for assessment of depletion due to the follow up measurement by Ag-DIOS MSI. Figure 2 shows three ion intensity maps for selected known compounds (no intensity normalization) for DIOS MSI analyses of the fingermark halves from the two independent samples. The detected ions included *m/z* 522 (Fig. 2a), *m/z* 550 (Fig. 2b) and *m/z* 827 (Fig. 2c). I*n situ* MS/MS was used to tentatively assign the identity of these three fingermark ions as ditallow dimethyl ammonium (DTDMA) C_{16}/C_{16}, DTDMA C_{18}/C_{18}, and TAG 48:1 (Fig. S1, Supporting Information). DTDMACs are commonly found in detergents and disinfectants[29], while TAGs are typical components of finger secretions (i.e. sebum). The TAG distribution across the first fingermark (left half in Fig. 2c) appeared to fade along the length of the fingermark, suggesting uneven contact pressure between the finger and the substrate during contact deposition. No such intensity fade was noticed for the independent replicate, and both analyses still allowed for detection of the selected ions.

Following the initial round of MSI analyses, the same two DIOS substrates were sputter-coated with a 1-2 nm thick layer of Ag and the entire fingermark was re-analyzed. Application of Ag in this way has three important effects on subsequent MSI. First, as demonstrated previously, Ag allows for LDI in the absence of an underlying DIOS substrate: an observation that has been independently demonstrated previously [13]. Secondly, a series of Ag clusters is introduced across the mass range measured [23]. Finally, Ag forms adducts with specific compounds (e.g. cholesterol), which can otherwise be difficult to detect [3, 13].

Figure 2 (here)

The stark differences between the DIOS and Ag-DIOS average spectra (Fig. S2, Supporting Information) made direct comparison of the entire data sets difficult. Thus, a targeted comparison of known fingermark compounds was employed to highlight the complementarity of the MSI data acquired on Ag-DIOS.

This targeted analysis employed the drastically improved mass accuracy afforded by internal calibration using the Ag isotopomers present in the Ag-DIOS MSI analysis [22], thus increasing confidence in matching mass values to putative compound identities: (outlined in Fig. S3, Supporting Information, and Table 1 [22]. Figures 2d and 2e present ion maps for oleic acid (i/iii, no adduct *m/z* 283.263 / +Ag *m/z* 389.160), stearic acid (ii/iv, no adduct *m/z* 285.279 / +Ag *m/z* 391.176) and a WE (WE 36:1) [v/vi, no adduct *m/z* 557.527 / +Ag *m/z* 641.442]. Data for the second fingermark is shown in Fig. S4 (Supporting Information). Oleic acid, stearic acid and WE 36:1 were not detected on DIOS (Fig. 2d). In sharp contrast, Ag-adducted oleic acid, stearic acid and WE 36:1 exhibited clear localisation to the fingermark ridge (Fig. 2e), and detection was subsequently confirmed by inspection

of individual spectra. Given the significant signal intensity for these adducted compounds on Ag-DIOS, DIOS alone does not appear to be an appropriate substrate for FA detection. Indeed, a control experiment with a stearic acid standard (500 ng/mL), confirmed that this FA was only readily detectable as a Ag adduct (Fig. S5, Supporting Information).

As the same sample was interrogated twice by MSI, analyte depletion was also evaluated. First, DIOS MSI was performed on half of each deposited fingermark. Subsequently, Ag-DIOS MSI data was acquired across the entire fingermark and the ion intensity maps for Ag-adducted oleic acid (*m/z* 389.1604) were compared, demonstrating no observable depletion (Fig. S6, Supporting Information). This was despite co-localization of MSI acquisition locations (Fig. S7, Supporting Information).

Fingermark MSI on Ag-DIOS was able to provide an additional tier of information for compounds such as FAs which are not readily detected using DIOS alone. DIOS/Ag-DIOS MSI may therefore hold considerable promise for application in spatial metabolomics. To assess this, the next step was to test the translatability of this method to animal tissues, with a focus on applications in pharmacokinetics. More specifically, in animal models, absorption-distribution-metabolism-excretion (ADME) analysis requires improved detection of drug metabolites in complex mammalian organ systems, as these compounds are typically difficult to extract and characterize. It was hypothesized that DIOS/Ag-DIOS could achieve this and add spatial information for endogenous small molecules, thereby supporting integration of this MSI method into spatial metabolomics. A putative chemo-preventative compound, 6-bromoisatin [30] was thus studied in an established colorectal chemo-preventative azoxymethane (AOM) model. AOM is an intraperitoneal administered pro-carcinogen that recapitulates the human colorectal cancer stages of initiation and progression in a mouse model [31]. After a two week acclimatization period, mice are administered six weekly injections of the pro-carcinogen followed by six weeks of no injections to allow tumour precursors, aberrant crypt foci (ACF), and tumors to develop in the colon prior to sacrifice. The AOM model is effective at evaluating the chemo-preventative properties of drug candidates as the model is highly reproducible and experimental drugs can be effectively evaluated against well-established equivalents, or histopathological changes in colon tissue. AOM undergoes hepatic and gastrointestinal metabolism to form the carcinogenic compound methylazoxymethanol, which forms adducts on DNA nucleotides [32]. Candidate drugs can therefore be administered in the intended delivery mode, for example orally, without influencing the administration of the carcinogen.

6-bromoisatin is actively processed to yield several metabolites, including the dimer 6,6'-dibromoindirubin (6,6'-DBI), a known constituent of Tyrian purple (*m/z* 419, Table 1). Mice were administered a daily oral gavage with 6-bromoisatin across a 14 week model and tissues were excised four hours after the last treatment [30]. Sections were obtained from the fore-stomach of a treated mouse and mounted onto a DIOS substrate to allow adsorptive transfer (imprinting) of analytes prior to physical removal of the section by rinsing [26, 27] and DIOS/Ag-DIOS MSI.

DIOS MSI indicated that the levels of 6-bromoisatin in the fore-stomach were low (see average spectra in Fig. S8 (Supporting Information), single spectra in Fig. S9 (Supporting Information) and control DIOS MS acquisitions for 6-bromoisatin in Fig. S10 (Supporting Information), a likely consequence of molecular dimerization in the gastrointestinal environment [33]. Indeed, singly protonated 6,6'-DBI, a known dimer and likely metabolite of 6-bromoisatin, was successfully detected as an ion cluster centred at *m/z* 421, with a theoretical isotopic distribution matching that expected. It should be noted that the isomer 6,6'-dibromoindigo (6,6'-I) can also form from natural extracts alongside 6,6'-DBI. For the purposes of this study 6,6'-DBI was annotated as a dimerization product of 6-bromoisatin, as it was considered unlikely that 6,6'-I would form *in vivo* from synthetic 6-bromoisatin. Unambiguous identification would require NMR, as 6,6'-DBI is isobaric with 6,6'-I.

Figure 3 highlights 6,6'-DBI as a high intensity peak cluster in a single DIOS MSI spectrum example (Fig. 3 – unformatted spectra in Fig. S11/S12, Supporting Information). Peak identity was confirmed by matching the expected isotopic distribution to that observed in the individual spectra (Fig. 3 inset). These dimeric metabolites can have markedly different bioactive properties from the administered compound [33]. The detection of this brominated dietary metabolite of 6-bromoisatin was ideal for demonstrating the targeted MSI mapping for metabolites of interest, which are easily identifiable in the MS data due to their characteristic isotopic profile.

Figure 3.

As outlined by the ion intensity maps for both DIOS MSI (Fig. 4a) and Ag-DIOS MSI (Fig. 4d), 6,6'-DBI was detected and spatially annotated as punctate foci within the murine fore-stomach. Median normalization was used for the data presented here: for a comparison of the effect of normalization strategies, see Fig. S13 (Supporting Information). Mean and skyline spectra (no averaging of ions detected in small numbers of spectra) also clearly showed 6,6'-DBI in the MSI data for both DIOS and Ag-DIOS measurements (Fig. S8, Supporting Information) and, as demonstrated in Fig. 3, 6,6'-DBI was detected at high intensity within these foci using DIOS MSI. Successful additional detection of this ion by Ag-DIOS MSI, and internal calibration using Ag clusters, also increased the mass accuracy significantly. 6,6'-DBI was thus assigned by combining improved accuracy with its unique isotopic envelope, which matches that from DIOS MS measurement of muricid mollusc extracts known to contain both 6-bromoisatin and its dimers (Fig. S10, Supporting Information).

In terms of biological context, the majority of the detected 6,6'-DBI foci appeared to be localized to the stomach lumen. The dimerization of 6-bromoisatin into 6,6'-DBI provided a good model of drug bio-distribution because of the distinctive spectral pattern of di-brominated compounds, but also since the dimer has low solubility and thus predictably remained in the lumen environment.

By combining both MSI modes with LC/MS and comparison with the reviewed literature [35], tentative phospholipid identities for mapped ions could be proposed. Ion intensity maps for these lipids were manually selected, in contrast to using the theoretical *m/z* values, to compensate for the *m/z* error in the externally-calibrated DIOS MSI data. This allowed mapping of the ion peak maxima for *m/z* 758.777 and *m/z* 782.772 in Figs. 4b and 4c, respectively. These ions could be tentatively assigned as phosphatidylcholine PC(34:2) [reported *m/z* 758.5] and PC(36:4) [reported *m/z* 782.6], respectively [35]. The assignment of these masses was supported by LC/MS of murine stomach lipid extracts from the same mouse model (LC/MS in Figs. S14a-c (Supporting Information) showing detected *m/z* values of 758.6 and 782.6). Furthermore, the PC identity of the *m/z* values in this mass range was supported by the detection of the PC head group in MALDI-ToF/ToF MS/MS spectra for *m/z* 756.477 and 780.486 following thin-layer chromatography (TLC) separation (Figs. S14d-f, Supporting Information). These assignments are tentative and further work is needed to confidently assign the identity of these and other lipids present in the forestomach tissues.

For Ag-DIOS MSI, Ag-adducted ions matching in mass to oleic (Fig. 3, Fig. 4e, *m/z* 389.160) and stearic acid (Table 1) as well as prostaglandin (Fig. S15, Supporting Information) and cholesterol (Table 1, Fig. 4f, and Fig. S15 (Supporting Information)) [13] could be detected and mapped to the lumen and mucosal layers. The detection of FAs in these data could be the result of lipase activity or fragmentation of glycerolipids during ionisation. This is worth investigating in future work, as intact TAGs were detected in fingermarks (see Table 1). Furthermore, the full extent of lipid detection using the DIOS/Ag-DIOS MSI platform needs to be characterized, ideally through a combination of LC/MS and high mass accuracy lipid profiling on DIOS (e.g. MALDI-FTICR).

These results were considered in the context of both an optical scan of tissue prior to the rinse removal and MSI analysis (Fig. 4g) as well as a haematoxylin and eosin stained tissue section from the same sample block (Fig. 4h). Indeed, these results indicated that 6,6'-DBI could be placed in the context of both lipid distributions (Figs. 4b/c/e/f) and murine fore-stomach histology (Figs. 4g/h). The latter contention was further supported by the results of hierarchical clustering (Fig. 4i) and probabilistic latent semantic analysis (pLSA, Fig. 4j-n, Supporting Information) [36] for the Ag-DIOS MSI data. Indeed, the histology highlighted here by both manual (ion maps) and automated (clustering) data analysis are particularly important for stomach tissue, as the differentiation of the gastrointestinal lumen from mucosa shows the spatial distinction between a very low pH environment and physiologically neutral surrounding tissue. Indole structures in particular undergo dimerization at low pH. Thus, detecting the effects of acidity on orally administered compounds requires this level of spatial distinction.

Figure 4.

To summarize, the DIOS/Ag-DIOS MSI approach could easily detect and spatially map 6,6'-DBI, a non-polar secondary metabolite which is very difficult to extract in most organic solvents [37]. Direct analysis by MSI thus circumvents lengthy and potentially destructive extraction processes to capture a metabolite class that is typically under-represented in solvent extraction profiles, while also capturing the spatial distribution. Secondly, simultaneous detection of secondary metabolites, such as brominated indoles, with primary metabolites such as lipids could be a major advantage for assessment of drug metabolism and steatosis (fatty change). Further annotation of the complex ion set detected will determine the suitability of the combined MSI method for specific lipid classes, such as sterols and phospholipids. By comparison, traditional lipid analysis approaches require multiple derivatization steps and analytical platforms to detect these compound classes [37]. Thirdly, the ability to detect metabolites with MSI on both DIOS and Ag-DIOS could enable re-calibration of DIOS spectra by aligning the masses which exist in both. Here, the mass error for the AWM 6,6'-DBI *m/z* 418.9121 peak (Table 1 and Fig. S16, Supporting Information) was only 22.92 ppm from the theoretical *m/z* value. The AWM *m/z* errors for 6,6'-DBI, FAs and cholesterol were thus all below 25 ppm, demonstrating the excellent mass accuracy of this MSI technique (Table 1), compared with externally calibrated MSI by MALDI-ToF/ToF, and supporting the implementation of suitable spectral alignment tools to re-calibrate DIOS MSI data. Finally, consecutive use of two MSI approaches to clearly discriminate the gastrointestinal lumen and mucosa in the bio-imprint from a single tissue section, is suitable for discovering active metabolites, informing drug design and allowing pharmacokinetics to be spatially determined in preclinical animal models for new drug development.

Future work should further complement the presented DIOS/Ag-DIOS approach - first, by addressing the currently challenging co-registration of MSI data and histology. This would be aided by the future implementation of fiducial markers in the sectioned tissue block, to allow alignment of introduced, and therefore known, spatial markers [38]. Ultimately, the aim should be the further adaptation of DIOS/Ag-DIOS to allow direct analysis of tissue (i.e. no rinse removal). Secondly, further work would be strengthened by exhaustive chemo-informatics, such as Ag-based mass defect filtering [39] and adduct/fragmentation analyses [40]: this is supported by the sheer number of potential additional ions detected (Fig 3; highlighted area). The further annotation of these ions will establish precisely how additive these two MSI levels are when overlaid. Finally, targeted LC/MS/MS will provide future studies with exhaustive identity annotation, and translation to high mass accuracy MS systems

(e.g. FTICR/Orbitrap) will provide the exact masses required for the aforementioned defect/adduct analyses. The spatial information gained with DIOS/Ag-DIOS MSI provides molecular specificity not normally obtained with traditional dye-based histochemistry routinely used in the pathological evaluation of damaged tissue, in particular for lipids in diseased tissues [41]. DIOS/Ag-DIOS could therefore contribute to molecular histology, both as an orthogonal tool to lipid histochemical analyses that lack *a priori* knowledge of significantly altered lipid species, and also as a discovery platform in drug models of disease.

CONCLUDING REMARKS

By mapping known fingermark ions and brominated metabolites in conjunction with lipids and Ag-adductable small molecules that are difficult to detect on DIOS alone, this study has demonstrated, for both fingermarks and tissue sections, that bimodal DIOS/Ag-DIOS is a powerful addition to the MSI toolbox. Crucially, this novel approach exhibits minimal observable depletion, as demonstrated for the fingermark data, and is a first step to achieving overlay of multi-omics MSI data from nanostructured substrates with tissue morphology: it should therefore directly supplement traditional histochemistry approaches. This straightforward MSI method has the potential to simplify the analysis of multiple compound classes from materially limited samples by using a single analytical platform to acquire multi-tiered spatial data sets. Future work linking these high dimensional MSI data sets to high mass accuracy MSI and LC/MS/MS will allow for a drastic increase in analytical depth.

ACKNOWLEDGEMENTS

The authors acknowledge Catherine Abbott and Babak Esmaeelian for provision of the animal model tissue. This research was funded by the Australian Research Council (ARC) Centre of Excellence in Convergent Bio-Nano Science and Technology (Project No. CE140100036) and an ARC Linkage Project (LP110020044). The authors thank Bruker Daltonics for the custom flexAnalysis script and acknowledge the Australian Microscopy & Microanalysis Research Facility at Flinders University.

REFERENCES

[1] R. M. Caprioli, T. B. Farmer, J. Gile. Molecular imaging of biological samples: localization of peptides and proteins using MALDI-TOF MS. *Anal. Chem.* **1997**, *69*, 4751.

[2] G. J. Patti, L. P. Shriver, C. A. Wassif, H. K. Woo, W. Uritboonthai, J. Apon, M. Manchester, F. D. Porter, G. Siuzdak. Nanostructure-initiator mass spectrometry (NIMS) imaging of brain cholesterol metabolites in Smith-Lemli-Opitz syndrome. *Neuroscience* **2010**, *170*, 858.

[3] G. J. Patti, H. K. Woo, O. Yanes, L. Shriver, D. Thomas, W. Uritboonthai, J. V. Apon, R. Steenwyk, M. Manchester, G. Siuzdak. Detection of carbohydrates and steroids by cation-enhanced nanostructure-initiator mass spectrometry (NIMS) for biofluid analysis and tissue imaging. *Anal. Chem.* **2010**, *82*, 121.

[4] O. J. Gustafsson, J. S. Eddes, S. Meding, S. R. McColl, M. K. Oehler, P. Hoffmann. Matrix-assisted laser desorption/ionization imaging protocol for in situ characterization of tryptic peptide identity and distribution in formalin-fixed tissue. *Rapid Commun. Mass Spectrom.* **2013**, *27*, 655.

[5] S. Meding, K. Martin, O. J. Gustafsson, J. S. Eddes, S. Hack, M. K. Oehler, P. Hoffmann. Tryptic peptide reference data sets for MALDI imaging mass spectrometry on formalin-fixed ovarian cancer tissues. *J. Proteome Res.* **2013**, *12*, 308.

[6] T. Guinan, C. Della Vedova, H. Kobus, N. H. Voelcker. Mass spectrometry imaging of fingerprint sweat on nanostructured silicon. *Chem. Commun.* **2015**, *51*, 6088.
[7] N. Lauzon, M. Dufresne, V. Chauhan, P. Chaurand. Development of Laser Desorption Imaging Mass Spectrometry Methods to Investigate the Molecular Composition of Latent Fingermarks. *J. Am. Soc. Mass Spectrom.* **2015**, *26*, 878.
[8] S. A. Schwartz, M. L. Reyzer, R. M. Caprioli. Direct tissue analysis using matrix-assisted laser desorption/ionization mass spectrometry: practical aspects of sample preparation. *J. Mass Spectrom.* **2003**, *38*, 699.
[9] L. S. Eberlin, X. Liu, C. R. Ferreira, S. Santagata, N. Y. R. Agar, R. G. Cooks. DESI then MALDI mass spectrometry imaging of lipid and protein distributions in single tissue sections. *Anal. Chem.* **2011**, *83*, 8366.
[10] R. T. Steven, J. Bunch. Repeat MALDI MS imaging of a single tissue section using multiple matrices and tissue washes. *Anal. Bioanal. Chem.* **2013**, *405*, 4719.
[11] E. J. Lanni, R. N. Masyuko, C. M. Driscoll, J. T. Aerts, J. D. Shrout, P. W. Bohn, J. V. Sweedler. MALDI-guided SIMS: multiscale imaging of metabolites in bacterial biofilms. *Anal. Chem.* **2014**, *86*, 9139.
[12] M. Aichler, A. Walch. MALDI Imaging mass spectrometry: current frontiers and perspectives in pathology research and practice. *Lab. Invest.* **2015**, *95*, 422.
[13] M. Dufresne, A. Thomas, J. Breault-Turcot, J. F. Masson, P. Chaurand. Silver-assisted laser desorption ionization for high spatial resolution imaging mass spectrometry of olefins from thin tissue sections. *Anal. Chem.* **2013**, *85*, 3318.
[14] S. N. Jackson, K. Baldwin, L. Muller, V. M. Womack, J. A. Schultz, C. Balaban, A. S. Woods. Imaging of lipids in rat heart by MALDI-MS with silver nanoparticles. *Anal. Bioanal. Chem.* **2014**, *406*, 1377.
[15] J. Wei, J. M. Buriak, G. Siuzdak. Desorption-ionization mass spectrometry on porous silicon. *Nature* **1999**, *399*, 243.
[16] Z. Shen, J. J. Thomas, C. Averbuj, K. M. Broo, M. Engelhard, J. E. Crowell, M. G. Finn, G. Siuzdak. Porous silicon as a versatile platform for laser desorption/ionization mass spectrometry. *Anal. Chem.* **2001**, *73*, 612.
[17] T. R. Northen, H. K. Woo, M. T. Northen, A. Nordstrom, W. Uritboonthail, K. L. Turner, G. Siuzdak. High surface area of porous silicon drives desorption of intact molecules. *J. Am. Soc. Mass Spectrom.* **2007**, *18*, 1945.
[18] L. Canham. *Microporous Silicon*. Springer International Publishing, **2014**.
[19] S. Francese, R. Bradshaw, L. S. Ferguson, R. Wolstenholme, M. R. Clench, S. Bleay. Beyond the ridge pattern: multi-informative analysis of latent fingermarks by MALDI mass spectrometry. *Analyst* **2013**, *138*, 4215.
[20] N. Budimir, J. C. Blais, F. Fournier, J. C. Tabet. Desorption/ionization on porous silicon mass spectrometry (DIOS) of model cationized fatty acids. *J. Mass Spectrom.* **2007**, *42*, 42.
[21] L. Chen, B. Xie, L. Li, W. Jiang, Y. Zhang, J. Fu, G. Guan, Y. Qiu. Rapid and Sensitive LC–MS/MS Analysis of Fatty Acids in Clinical Samples. *Chromatographia* **2014**, *77*, 1241.
[22] T. M. Guinan, O. J. Gustafsson, G. McPhee, H. Kobus, N. H. Voelcker. Silver-coating for high mass accuracy imaging mass spectrometry of fingerprints on nanostructured silicon. *Anal. Chem.* **2015**, *87*, 11195.
[23] S. Owega, E. P. Lai. Silver cationization of thia fatty acids and esters in laser desorption/ionization time-of-flight mass spectrometry. *J. Mass Spectrom.* **1999**, *34*, 872.

[24] G. Shui, W. F. Cheong, I. A. Jappar, A. Hoi, Y. Xue, A. Z. Fernandis, B. K. Tan, M. R. Wenk. Derivatization-independent cholesterol analysis in crude lipid extracts by liquid chromatography/mass spectrometry: applications to a rabbit model for atherosclerosis. *J. Chromatogr. A* **2011**, *1218*, 4357.
[25] S. Daemen, M. A. van Zandvoort, S. H. Parekh, M. K. Hesselink. Microscopy tools for the investigation of intracellular lipid storage and dynamics. *Mol. Metab.* **2016**, *5*, 153.
[26] D. Rudd, M. Ronci, M. R. Johnston, T. Guinan, N. H. Voelcker, K. Benkendorff. Mass spectrometry imaging reveals new biological roles for choline esters and Tyrian purple precursors in muricid molluscs. *Sci. Rep.* **2015**, *5*, 13408.
[27] M. Ronci, D. Rudd, T. Guinan, K. Benkendorff, N. H. Voelcker. Mass spectrometry imaging on porous silicon: investigating the distribution of bioactives in marine mollusc tissues. *Anal. Chem.* **2012**, *84*, 8996.
[28] R. C. Team. R Foundation for Statistical Computing. Vienna, Austria, **2016**.
[29] G. B. Yagnik, A. R. Korte, Y. J. Lee. Multiplex mass spectrometry imaging for latent fingerprints. *J. Mass Spectrom.* **2013**, *48*, 100.
[30] B. Esmaeelian, C. A. Abbott, R. K. Le Leu, K. Benkendorff. 6-bromoisatin found in muricid mollusc extracts inhibits colon cancer cell proliferation and induces apoptosis, preventing early stage tumor formation in a colorectal cancer rodent model. *Mar. Drugs* **2014**, *12*, 17.
[31] M. De Robertis, E. Massi, M. L. Poeta, S. Carotti, S. Morini, L. Cecchetelli, E. Signori, V. M. Fazio. The AOM/DSS murine model for the study of colon carcinogenesis: From pathways to diagnosis and therapy studies. *J. Carcinog.* **2011**, *10*, 9.
[32] V. Megaraj, X. Ding, C. Fang, N. Kovalchuk, Y. Zhu, Q. Y. Zhang. Role of hepatic and intestinal p450 enzymes in the metabolic activation of the colon carcinogen azoxymethane in mice. *Chem. Res. Toxicol.* **2014**, *27*, 656.
[33] S. Q. Wang, L. S. Cheng, Y. Liu, J. Y. Wang, W. Jiang. Indole-3-Carbinol (I3C) and its Major Derivatives: Their Pharmacokinetics and Important Roles in Hepatic Protection. *Curr. Drug. Metab.* **2016**, *17*, 401.
[34] C. J. Cooksey. Tyrian Purple: 6,6'-Dibromoindigo and Related Compounds. *Molecules* **2001**, *6*, 736.
[35] K. A. Berry, J. A. Hankin, R. M. Barkley, J. M. Spraggins, R. M. Caprioli, R. C. Murphy. MALDI imaging of lipid biochemistry in tissues by mass spectrometry. *Chem. Rev.* **2011**, *111*, 6491.
[36] M. Hanselmann, M. Kirchner, B. Y. Renard, E. R. Amstalden, K. Glunde, R. M. Heeren, F. A. Hamprecht. Concise representation of mass spectrometry images by probabilistic latent semantic analysis. *Anal. Chem.* **2008**, *80*, 9649.
[37] K. Benkendorff. Natural product research in the Australian marine invertebrate Dicathais orbita. *Mar. Drugs* **2013**, *11*, 1370.
[38] N. Ogrinc Potocnik, K. Skraskova, B. Flinders, P. Pelicon, R. M. Heeren. Gold sputtered fiducial markers for combined secondary ion mass spectrometry and MALDI imaging of tissue samples. *Anal. Chem.* **2014**, *86*, 6781.
[39] L. Sleno. The use of mass defect in modern mass spectrometry. *J. Mass Spectrom.* **2012**, *47*, 226.
[40] N. G. Mahieu, J. L. Spalding, S. J. Gelman, G. J. Patti. Defining and Detecting Complex Peak Relationships in Mass Spectral Data: The Mz.unity Algorithm. *Anal. Chem.* **2016**.
[41] A. Mehlem, C. E. Hagberg, L. Muhl, U. Eriksson, A. Falkevall. Imaging of neutral lipids by oil red O for analyzing the metabolic status in health and disease. *Nat. Protoc.* **2013**, *8*, 1149.

Table 1. Ions from selected compounds mapped on a single fingermark and tissue section using Ag-DIOS.

Sample	Compound	Ion	Theoretical mass[a]	*m/z* replicate 1[b]	*m/z* replicate 2[b]	Error (ppm)[c]
Fingermark	Behentrimonium	$C_{25}H_{54}N$	368.4251	368.4334	368.4369	27.28
	Oleic acid	$C_{18}H_{34}O_2Ag$	389.1604	389.1621	389.1634	6.04
	Stearic acid	$C_{18}H_{36}O_2Ag$	391.1761	391.1732	391.1726	8.18
	DTDMA (C_{16}/C_{16})	$C_{34}H_{72}N$	494.5659	494.5759	494.5814	25.78
	DTDMA (C_{16}/C_{18})	$C_{34}H_{76}N$	522.5972	522.6083	522.6149	27.55
	DTDMA (C_{18}/C_{18})	$C_{38}H_{80}N$	550.6285	550.6413	550.6488	30.06
	WE 36:1	$C_{36}H_{70}O_2Ag$	641.4421	641.4457	641.4530	11.30
	TAG 48:1	$C_{51}H_{96}O_6Na$	827.7099	827.7519	827.7460	47.18
Tissue section	PC head group	$C_5H_{15}PO_4N$	184.0733	184.1074		185.25
	Oleic acid	$C_{18}H_{34}O_2Ag$	389.1604	389.1668		16.45
	Stearic acid	$C_{18}H_{36}O_2Ag$	391.1761	391.1784		5.88
	6,6'-Dibromoindirubin (Tyrian purple)	$C_{16}H_9Br_2N_2O_2$	418.9025	418.9121		22.92
	Cholesterol	$C_{27}H_{46}OAg$	493.2594	493.2631		7.50

[a] compass IsotopePattern *m/z* value [b] internally calibrated abundance weighted mean (AWM) *m/z* value. [c] average absolute error from available replicate(s).

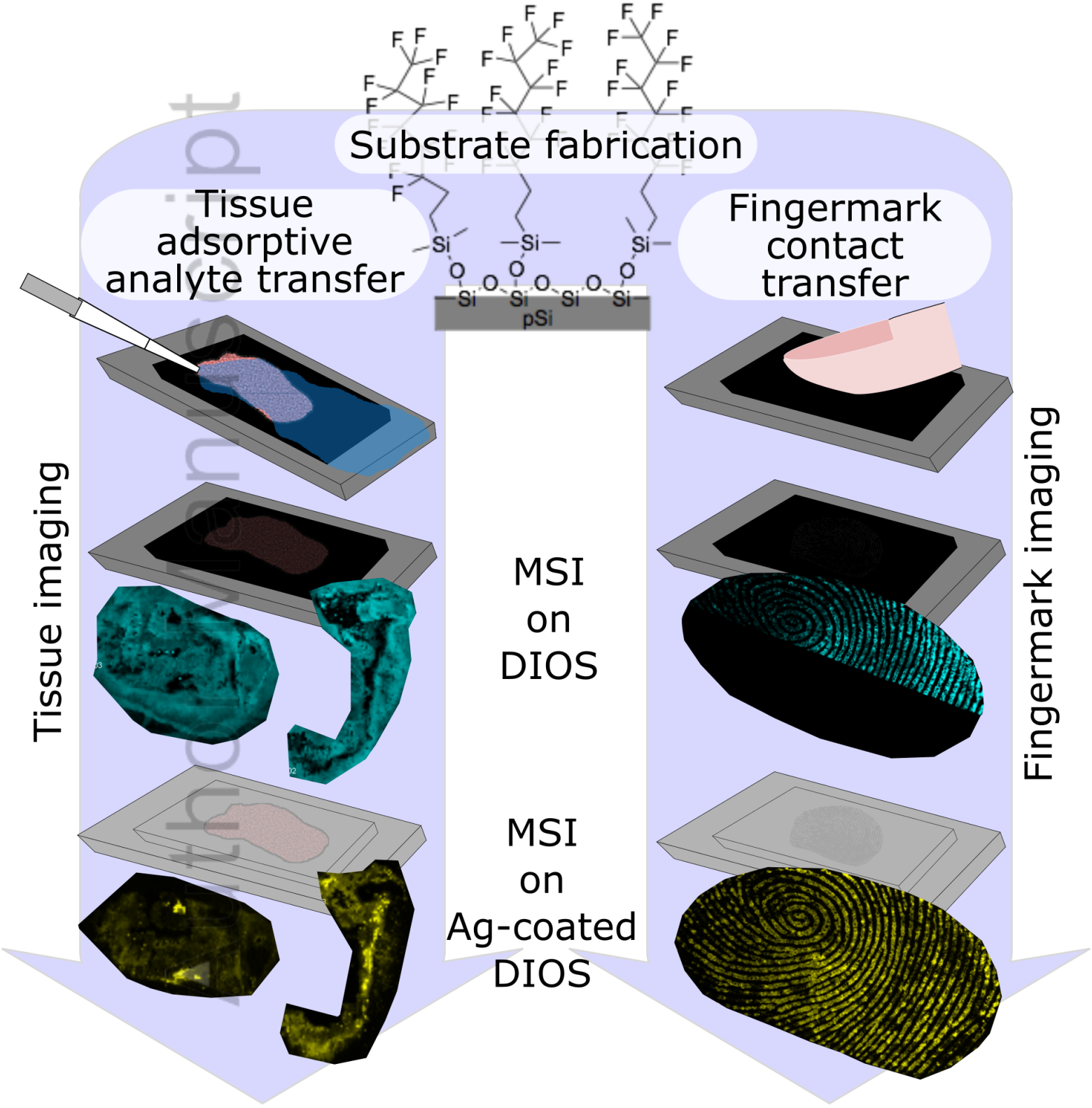

RCM_7869_F1.tif

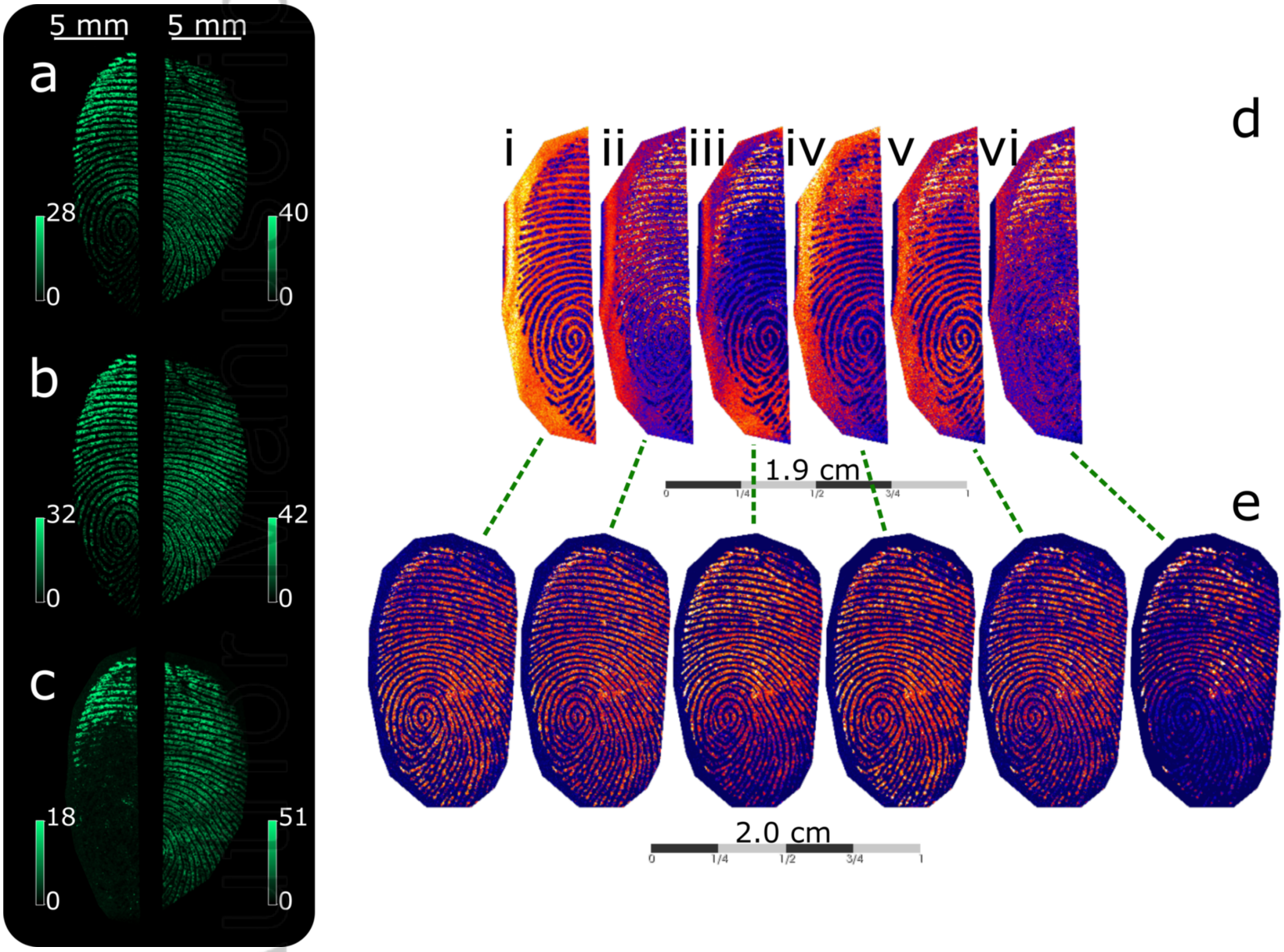

RCM_7869_F2.tif

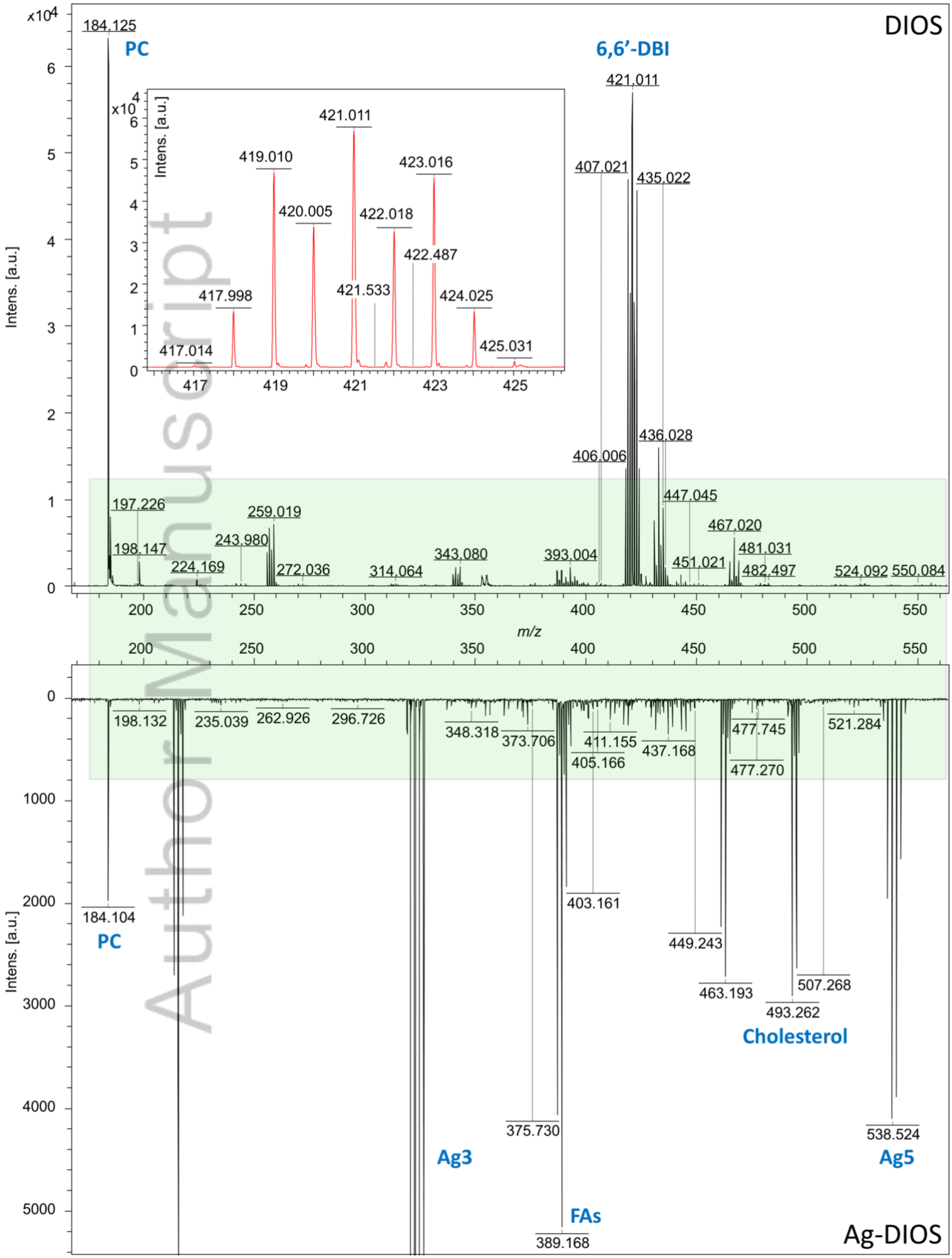

RCM_7869_F3.tif